J. Am. Chem. Soc. **1987**, *109*, 141-148

Molybdenum Carbonyl Derivatives of Catenated Rings and Chains of CH_3As and C_6H_5As Units. The Synthesis and Structural Characterization of [*cyclo*-$(CH_3As)_{10}Mo_2(CO)_6$], [*cyclo*-$(C_6H_5As)_9Mo_2(CO)_6$], and [*catena*-$(C_6H_5As)_8Mo_2(CO)_6$]

Arnold L. Rheingold,* Mark E. Fountain, and Anthony-J. DiMaio

Contribution from the Department of Chemistry, University of Delaware, Newark, Delaware 19716. *Received July 25, 1986*

Abstract: Reactions of the molybdenum carbonyls, $Mo(CO)_6$ and (mesitylene)$Mo(CO)_3$, with the homoatomic ring compounds *cyclo*-$(RAs)_n$ ($R = CH_3$, $n = 5$; $R = C_6H_5$, $n = 6$), in sealed tubes in toluene, have produced mixed main-group, transition-metal clusters containing from eight to ten catenated RAs units coordinated to two $Mo(CO)_3$ groups as *fac*-$[Mo(CO)_3L_3]$ complexes. Neither the products nor yields were significantly dependent on which metal precursor was used, but they were strongly dependent on R. From reactions with *cyclo*-$(CH_3As)_5$, in the absence of O_2, the only isolable product is [*cyclo*-$(CH_3As)_{10}Mo_2(CO)_6$] (**1**) containing a ten-membered CH_3As ring in a boat–chair–boat conformation; if all 12 heavy atoms are considered, the overall structure is a tetra edge-substituted cubane derivative. **1**: orthorhombic, *Pnnm*, $a = 15.689$ (3) Å, $b = 9.576$ (3) Å, $c = 11.097$ (3) Å, $V = 1667.1$ (7) Å^3, $Z = 2$, $R_F = 4.39\%$. In reactions with *cyclo*-$(PhAs)_6$, several cluster products are obtained depending on conditions. Two of these products are reported here. At 70 °C, the major product is [*cyclo*-$(PhAs)_9Mo_2(CO)_6$] (**2**) which contains a nine-membered ring of PhAs units in one of the stable cyclononane conformations. Overall, the eleven heavy atoms adopt a trishomocubane structure. **2**: monoclinic, $P2_1/c$, $a = 13.487$ (7) Å, $b = 18.784$ (7) Å, $c = 25.896$ (10) Å, $\beta = 94.41$ (3)°, $V = 6489$ (3) Å^3, $Z = 4$, $R_F = 6.38\%$. Neither **1** nor **2** have Mo–Mo bonds. At 120 °C in toluene, **2** is converted to [*catena*-$(PhAs)_8Mo(CO)_6$] (**3**); **3** may also be prepared directly from (mesitylene)$Mo(CO)_3$ and *cyclo*-$(PhAs)_6$ at the same temperature. **3** contains an eight-membered chain of PhAs units metal bonded in the 1, 4, 5, and 8 positions with its termini bridging both Mo atoms which are bonded, Mo–Mo = 3.094 (2) Å. **3**: monoclinic, $P2_1/n$, $a = 13.304$ (4) Å, $b = 19.654$ (4) Å, $c = 21.599$ (6) Å, $\beta = 100.25$ (3)°, $V = 5558$ (3) Å^3, $Z = 4$, $R_F = 6.95\%$.

The reactions of transition-metal carbonyls with cyclopolyarsines, *cyclo*-$(RAs)_n$, continue to be of great interest to us for two reasons: the cluster products are diverse and difficult to predict, and their high nuclearity structures often contain unprecedented constructions. From the initial ring structures of *cyclo*-$(RAs)_n$ ($n = 4$–6), products are formed containing coordinated rings of five to nine RAs units,[1a–c] or chains of four to eight RAs units with the termini acting as μ_2-bridging groups.[1a,2] Additionally, the organic group, R, may be lost, even under comparatively mild reaction conditions, to form complexes with single As atom bridges[3] or associated to form chains and rings of up to five naked As atoms.[3b,c,4]

Our prior experience with mixed main-group, transition-metal clusters suggests that the assemblage of stable clusters from metal and main-group construction units is primarily controlled by the steric and electronic requirements of the metallic fragment which is usually a 12–15 electron carbonyl and/or cyclopentadienyl moiety. In the presence of a ring-opening reagent (e.g., a metal carbonyl), *cyclo*-$(RAs)_n$ species enter into complex, dynamic reorganization equilibria producing a size array of ring and chain As–As bonded species.[1d] The comparatively inert metal fragment selects from this main-group melange those parts which best satisfy its requirements. Given the multitude of pathways that exist for such clusterification processes, the concept of a reaction mechanism as a specifiable sequence of steps is inappropriate.

We have previously reported products formed from $[\eta^5\text{-}C_5H_5Mo(CO)_3]_2$ and *cyclo*-$(PhAs)_6$[4a] or *cyclo*-$(CH_3As)_5$.[2a,4b] Our current report results from an investigation of the reactions of these same *cyclo*-$(RAs)_n$ species with $Mo(CO)_6$ and (mesitylene)$Mo(CO)_3$. One of the products formed from $Mo(CO)_6$ and *cyclo*-$(PhAs)_6$ is mononuclear, [*cyclo*-$(PhAs)_6Mo(CO)_4$], and has been described in an earlier report.[5]

Experimental Section

General Procedures. All reactions and manipulations were carried out under an atmosphere of purified N_2 or in evacuated (Carius) tubes. Melting points were measured on a Mel-Temp apparatus and are uncorrected. Infrared (IR) spectra were recorded on a Nicolet 50XB FTIR spectrophotometer as KBr pellets or as solutions in either CH_2Cl_2 or toluene. ^1H NMR spectra were obtained on a Bruker 250 MHz spectrometer with Me_4Si as an internal reference. All new compounds provided satisfactory elemental analyses and are air stable as solids.

Materials. Toluene was freshly distilled from sodium benzophenone ketyl under N_2. $Mo(CO)_6$ (Aldrich) was sublimed before use. *cyclo*-$(MeAs)_5$,[6] *cyclo*-$(PhAs)_6$,[7] and (mesitylene)$Mo(CO)_3$[8] were prepared by published procedures.

Preparation of [*cyclo*-$(MeAs)_{10}Mo_2(CO)_6$] (1). $Mo(CO)_6$ (0.31 g, 1.17 mmol) was dissolved in 10 mL of a dry, degassed toluene solution containing 1.10 g (2.44 mmol) of *cyclo*-$(CH_3As)_5$ in a medium-wall Carius tube. The tube was evacuated with 3 freeze–pump–thaw cycles, flame sealed, and heated at 120 °C for 48 h in an oven. (CAUTION: Carius tube pressures may reach 20–30 atm under these conditions; all heating should be done only after placing the sealed tube in an end-capped, perforated steel tube.) On slow cooling to room temperature, canary-yellow crystals of **1** formed in good yield (60%) and were collected by filtration. **1**: mp = 180 °C darkens, 295 °C dec; ^1H NMR;[10b] IR $\nu(CO)$ 1927(s), 1868 (m), 1844 (s) cm^{-1}.

Preparation of [*cyclo*-$(PhAs)_9Mo_2(CO)_6$] (2). (Mesitylene)$Mo(CO)_3$ (0.29 g, 0.96 mmol) and *cyclo*-$(PhAs)_6$ (0.46 g, 0.44 mmol) were dissolved in 6.0 mL of toluene and sealed, as above, in a Carius tube (see

---

(1) (a) Elmes, P. S.; West, B. O. *Aust. J. Chem.* **1970**, *23*, 2247. (b) Elmes, P. S.; Gatehouse, B. M.; West, B. O. *J. Organomet. Chem.* **1974**, *82*, 235. (c) Elmes, P. S.; Gatehouse, B. M.; Lloyd, D. J.; West, B. O. *J. Chem. Soc., Chem. Commun.* **1974**, 953. (d) Rheingold, A. L. In *Homoatomic Rings, Chains and Macromolecules of the Main-Group Elements*; Rheingold, A. L., Ed.; Elsevier: Amsterdam, 1977; p 385.

(2) (a) Rheingold, A. L.; Churchill, M. R. *J. Organomet. Chem.* **1983**, *243*, 165. (b) Gatehouse, B. M. *J. Chem. Soc., Chem. Commun.* **1969**, 948.

(3) (a) Rheingold, A. L.; Sullivan, P. J. *J. Chem. Soc., Chem. Commun.* **1983**, 39. (b) Foust, A. S.; Foster, M. S.; Dahl, L. F. *J. Am. Chem. Soc.* **1969**, *98*, 5631, 5633. (c) Di Vaira, M.; Midollini, S.; Sacconi, L.; Zanobini, F. *Angew. Chem., Int. Ed. Engl.* **1978**, *17*, 676. Hermann, W. A. *Angew. Chem., Int. Ed. Engl.* **1986**, *25*, 56.

(4) (a) Sullivan, P. J.; Rheingold, A. L. *Organometallics* **1982**, *1*, 1547. (b) Rheingold, A. L.; Foley, M. J.; Sullivan, P. J. *J. Am. Chem. Soc.* **1982**, *104*, 4727.

(5) Rheingold, A. L., Fountain, M. E. *Organometallics*, in press.

(6) Rheingold, A. L. *Organomet. Synth.* **1986**, *3*, 618.

(7) Palmer, C. S.; Scott, A. B. *J. Am. Chem. Soc.* **1928**, *50*, 536.

(8) Strohmeier, W. *Chem. Ber.* **1961**, *94*, 3337.

0002-7863/87/1509-0141$01.50/0

Table I. Crystal, Data Collection, and Refinement Parameters for **1**, **2**, and **3**

	1	**2**	**3**
formula	$C_{16}H_{30}As_{10}Mo_2O_6$	$C_{60}H_{45}As_9Mo_2O_6 \cdot 1/2\ C_2H_5OH$	$C_{54}H_{40}As_8Mo_2O_6$
crystal system	orthorhombic	monoclinic	monoclinic
space group	*Pnnm*	$P2_1/c$	$P2_1/n$
a, Å	15.689 (3)	13.487 (7)	13.304 (4)
b, Å	9.576 (3)	18.784 (7)	19.654 (4)
c, Å	11.097 (3)	25.896 (10)	21.599 (6)
β, deg		94.41 (3)	100.25 (3)
V, Å^3	1667.1 (7)	6489 (3)	5558 (3)
Z	2	4	4
μ(Mo Kα) cm^{-1}	106.0	49.8	52.8
D(calcd), g cm^{-3}	2.509	1.792	1.883
color	green-yellow	orange	orange-red
size, mm	0.20 × 0.20 × 0.38	0.30 × 0.32 × 0.36	0.09 × 0.45 × 0.45
temp, K	293	294	294
diffractometer	Nicolet R3m/μ	same	same
radiation	Mo Kα (λ = 0.71073 Å)	same	same
monochromator	graphite	same	same
scan limits, deg	$4 \leq 2\theta \leq 53$	$4 \leq 2\theta \leq 45$	$4 \leq 2\theta \leq 45$
scan speed, deg min^{-1}	var. 5–20	6	6
scan method	ω	ω	ω
std rflns	3 std/97 rflns	3 std/197 rflns	3 std/197 rflns
data collected	1989	8713	7569
unique data	1811	8182	6970
R(int), %		2.45	1.69
indepndt data ($n\sigma F_0$)	1295 (n = 4)	3462 (n = 5)	4522 (n = 3)
decay, %	≤1.3	≤1.5	≤3
R_F, R_{wF}, %	4.39, 5.15	6.38, 6.50	6.95, 7.15
GOF	1.51	1.55	1.43
N_o/N_v	15.2	10.6	8.4
$\Delta(\rho)$, e Å^{-3}	0.77	1.0	1.6
Δ/σ	0.05	0.08	0.06
g, ($w^{-1} = \sigma^2(F_o) + gF_o^2$)	0.001	0.001	0.002

CAUTION above). The tube was heated at 70 °C for 29 h. After being cooled to room temperature, the solution was filtered, and evaporated to dryness, and the solid residue was chromatographed on alumina (60/40 hexane/methylene chloride). Recrystallization from EtOH/$CHCl_3$ (1:1) solution yielded a bright orange solid (62%). **2**: mp 225–230 °C dec; IR ν(CO) 1940 (s), 1867 (br) cm^{-1}.

Preparation of [*catena*-(PhAs)$_8$Mo$_2$(CO)$_6$] (3). With use of methods similar to those for **2**, 2.09 g (6.97 mmol) of (mesitylene)Mo(CO)$_3$ and 6.00 g (6.58 mmol) of *cyclo*-(PhAs)$_6$ were heated in 20 mL of toluene at 120 °C for 67 h (see CAUTION above). After being cooled to room temperature, the tube was opened and filtered. The collected solid was washed with hexane and CH_2Cl_2 and dried, yielding 1.07 g (26%) of dark red needles. **3**: mp 245–250 °C dec; IR ν(CO) 1985, 1966, 1922, 1902, 1876 cm^{-1}.

Conversion of 2 to 3. A 0.45-g sample of **2** was sealed in a degassed Carius tube containing 10.0 mL of toluene and heated at 120 °C for 24 h. The solution was treated as above. A 72% yield of **3** was isolated and its identity established by determining that the unit-cell symmetry and parameters were identical with those for **3**.

X-ray Structural Determinations. Crystal, data collection, and refinement parameters are given in Table I. All specimens were affixed to glass fibers with epoxy cement; photographic and peak width criteria showed that all were of adequate, but moderate quality. Unit-cell parameters were obtained from the least-squares fit of the angular settings of 25 reflections (20° ≤ 2θ ≤ 30°) containing Friedel-related sets to check optical and diffractometer alignment. Systematic absences in the intensity data uniquely determined the space groups for **2** and **3** and indicated either *Pnnm* or *Pnn*2 for **1**. The centrosymmetric alternative was originally selected on the basis of the statistical distribution of $E^2 - 1$ values and was confirmed by the successful solution and well-behaved refinement of a chemically rational structure. Intensity data were collected to the limits of availability in 2θ. All data sets were corrected for *Lp* effects, **3** only for decay, and corrections for absorption were attempted both empirically (ψ-scan method) and by XABS.[9] Comparable results were obtained for **1** and **2**, but for **3**, which was a thin plate, XABS produced significantly superior results as evidenced by R factor (6.95% vs. 7.49%) and maximum residual electron density (1.6 vs. 2.2 e Å^{-3}).

Table II. Atomic Coordinates (×10^4) and Isotropic Thermal Parameters (Å^2 × 10^3) for **1**

	x	y	z	U
As(1)	9354 (12)	734 (1)	3295 (1)	40 (1)^a
As(2)	9072 (1)	−2454 (1)	5000	42 (1)^a
As(3)	10073 (1)	−3090 (1)	6595 (1)	46 (1)^a
Mo(1)	8323 (1)	−44 (1)	5000	41 (1)^a
O(1)	7324 (8)	2851 (12)	5000	40 (4)^a
O(2)	7041 (7)	−1151 (11)	3074 (13)	72 (5)^a
C(1)	7696 (11)	1882 (24)	5000	86 (8)^a
C(2)	7512 (7)	−749 (11)	3713 (15)	77 (5)^a
C(3)	8322 (10)	−4091 (17)	5000	66 (7)^a
C(4)	8965 (9)	727 (13)	1627 (12)	73 (5)^a
C(5)	9268 (9)	−3099 (15)	7959 (13)	83 (5)^a

^{a} Equivalent isotropic U defined as one-third of the trace of the orthogonalized U_{ij} tensor.

Structure solutions (direct methods, SOLV) and completions (difference Fourier syntheses) were straightforward. For **2** and **3** rigid, planar hexagonal body constraint was applied to the phenyl rings (d(C–C) = 1.395 Å). All non-hydrogen atoms for **1** and **3** were refined (blocked-cascade) anisotropically, and, for **2**, all non-hydrogen atoms except for those of the phenyl rings and a fractionally occupied molecule of EtOH were refined anisotropically. In all cases hydrogen atoms were treated as idealized, isotropic contributions by using a riding model (d(C–H) = 0.96 Å).

All software (except XABS) is contained in the SHEXLTX 4.1 program library (Nicolet XRD, Madison, WI) and was executed on a Data General S-30 computer.

Tables II, III, and IV give the atomic coordinates for **1**, **2**, and **3**, and Tables V, VI, and VII contain selected bond distances, angles, and torsion angles for **1**, **2**, and **3**. Additional crystallographic data are available as supplementary material (see the paragraph at the end of the paper).

Results

Arsenomethane, *cyclo*-(CH$_3$As)$_5$, reacts with either Mo(CO)$_6$ or (mesitylene)Mo(CO)$_3$ at 120 °C in toluene to produce [*cyclo*-(CH$_3$As)$_{10}$Mo$_2$(CO)$_6$] (**1**) in good yield. (The yields are similar for both metal precursors, but the lower ultimate pressurization of Carius tubes using (mesitylene)Mo(CO)$_3$ makes these reactions safer to run.) If dioxygen is admitted to either reaction,

---

[9] Hope, H.; Moezzi, B.: The method obtains an empirical absorption tensor from an expression relating F_0 and F_c; a copy of the unpublished program was obtained from the authors at the University of California—Davis.

Table III. Atomic Coordinates (×10^4) and Isotropic Thermal Parameters (Å^2 × 10^3) for **2**

	x	*y*	*z*	*U*		*x*	*y*	*z*	*U*
Mo(1)	1830 (2)	7280 (1)	2240 (1)	61 (1)^a	C(36)	3139	5152	892	87 (9)
Mo(2)	4336 (2)	7075 (1)	950 (1)	58 (1)^a	C(41)	535 (12)	5319 (9)	846 (6)	92 (9)
As(1)	3657 (2)	6857 (1)	2461 (1)	57 (1)^a	C(42)	−224	4810	762	106 (10)
As(2)	4138 (2)	5705 (1)	2130 (1)	62 (1)^a	C(43)	−875	4717	1129	121 (11)
As(3)	3303 (2)	6020 (1)	1266 (1)	60 (1)^a	C(44)	−767	5134	1580	105 (10)
As(4)	1648 (2)	6479 (1)	1420 (1)	63 (1)^a	C(45)	−8	5644	1664	87 (8)
As(5)	1317 (2)	7046 (2)	559 (1)	82 (1)^a	C(46)	643	5736	1297	70 (7)
As(6)	2735 (2)	7851 (1)	830 (1)	64 (1)^a	C(51)	−757 (17)	7168 (8)	701 (7)	142 (13)
As(7)	2423 (2)	8304 (1)	1687 (1)	64 (1)^a	C(52)	−1658	7521	728	131 (12)
As(8)	4160 (2)	8734 (1)	1926 (1)	70 (1)^a	C(53)	−1685	8263	735	131 (12)
As(9)	4734 (2)	7502 (1)	1918 (1)	57 (1)^a	C(54)	−811	8652	714	154 (14)
O(1)	1216 (14)	6163 (10)	3001 (7)	111 (9)^a	C(55)	90	8299	687	113 (11)
O(2)	1797 (16)	8308 (11)	3168 (8)	114 (11)^a	C(56)	117	7557	681	86 (8)
O(3)	−434 (12)	7702 (10)	1986 (8)	115 (10)^a	C(61)	3390 (13)	9113 (11)	378 (6)	113 (11)
O(4)	6231 (14)	6137 (11)	939 (7)	105 (10)^a	C(62)	3389	9646	2	155 (14)
O(5)	5668 (14)	8290 (10)	630 (7)	98 (9)^a	C(63)	2650	9653	−435	144 (13)
O(6)	3831 (17)	6692 (11)	−222 (7)	136 (11)^a	C(64)	1912	9127	−497	138 (13)
C(1)	1470 (17)	6550 (14)	2723 (9)	77 (11)^a	C(65)	1912	8594	−121	121 (11)
C(2)	1878 (18)	7939 (15)	2832 (11)	78 (13)^a	C(66)	2651	8588	316	92 (9)
C(3)	433 (21)	7579 (14)	2083 (12)	110 (14)^a	C(71)	2040 (11)	9760 (11)	1294 (7)	135 (13)
C(4)	5533 (21)	6476 (14)	964 (9)	74 (12)^a	C(72)	1539	10412	1253	169 (16)
C(5)	5141 (21)	7832 (16)	754 (10)	87 (13)^a	C(73)	753	10534	1537	109 (10)
C(6)	4064 (19)	6822 (13)	241 (9)	82(1)^a	C(74)	468	10003	1863	95 (9)
C(11)	3824 (9)	6886 (8)	3583 (7)	87 (9)	C(75)	969	9351	1904	92 (9)
C(12)	4286	6782	4096	99 (10)	C(76)	1755	9230	1620	77 (8)
C(13)	5275	6544	4194	105 (10)	C(81)	3551 (11)	9646 (8)	2716 (6)	86 (9)
C(14)	5804	6410	3780	119 (11)	C(82)	3423	9877	3214	93 (9)
C(15)	5342	6515	3267	96 (9)	C(83)	3759	9457	3648	92 (9)
C(16)	4353	6753	3169	68 (7)	C(84)	4222	8805	3585	103 (10)
C(21)	3630 (9)	4906 (8)	2967 (6)	75 (8)	C(85)	4350	8574	3088	83 (8)
C(22)	3070	4455	3242	91 (9)	C(86)	4014	8994	2653	70 (7)
C(23)	2125	4224	3012	89 (9)	C(91)	6515 (12)	7978 (7)	2654 (6)	96 (9)
C(24)	1739	4443	2507	99 (9)	C(92)	7476	7889	2929	89 (9)
C(25)	2299	4894	2233	70 (7)	C(93)	8034	7285	2846	103 (10)
C(26)	3244	5125	2463	56 (6)	C(94)	7630	6770	2488	95 (9)
C(31)	3353 (11)	4495 (11)	1134 (5)	85 (8)	C(95)	6669	6859	2212	81 (8)
C(32)	3283	3873	837	127 (12)	C(96)	6112	7463	2295	51 (6)
C(33)	2998	3908	298	123 (11)	O(7)^b	−156 (38)	2667 (27)	1125 (19)	180 (20)
C(34)	2784	4565	55	130 (12)	C(98)^b	437 (40)	2826 (30)	852 (20)	93 (18)
C(35)	2855	5187	353	121 (11)	C(99)^b	1000 (41)	2272 (31)	741 (21)	102 (19)

^{a}Equivalent isotropic *U* defined as one-third of the trace of the orthogonalized U_{ij} tensor. ^{b}Atoms forming molecule of EtOH.

the product is instead the arsaoxane complex, [*cyclo*-$(CH_3AsO)_6Mo_2(CO)_6]_2$ (**4**), containing a 12-membered alternating As–O ring.[10a] Using reagents and conditions closely related

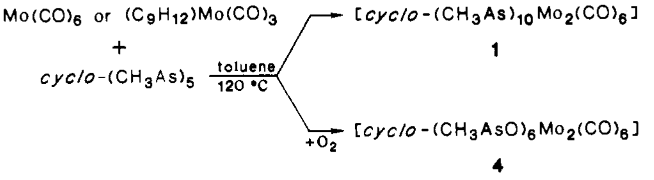

to our synthesis of **1**, West obtained a product which he originally formulated as $[Mo(CO)_4(CH_3As)_5]_2$,[1a] but later reformulated as [*cyclo*-$(CH_3As)_9Mo_2(CO)_6$] to correspond to the determined structure of [*cyclo*-$(CH_3As)_9Cr_2(CO)_6$].[1b] We now believe that West's product and **1** are identical and that **1** is a cyclodecamer complex. Minor differences in the spectral and elemental analysis data we and West report are explicable if West's sample is contaminated with small quantities of the arsaoxane complex, **4**.[10b] The unprecedented structure of the cyclodecamer complex **1** is shown in Figures 1 and 2. The molecule is centered on a site with *mm* symmetry with $^1/_4$ of the molecule being crystallographically unique. The ten-membered ring of CH_3As units, which is coordinated to two $Mo(CO)_3$ groups by using the 1, 2, 4, 6, 7, and 9 ring atoms, is highly puckered and closely resembles the ground-state, boat–chair–boat conformation of cyclodecane;[11] an Mo⋯Mo distance of 5.263 (1) Å precludes metal–metal bonding.

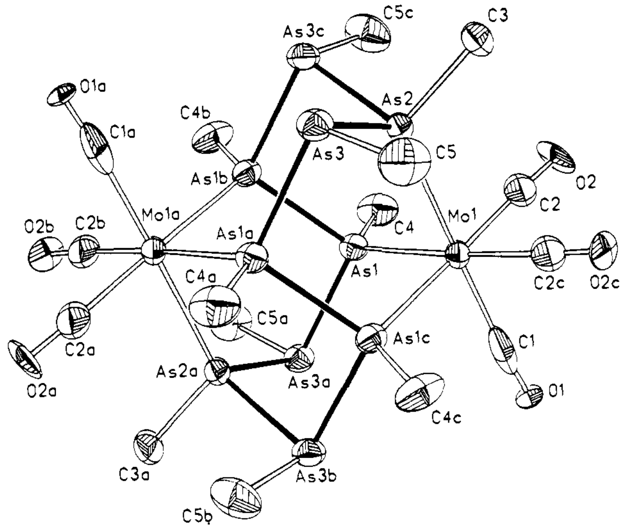

Figure 1. Molecular structure and labeling scheme for **1**.

---

(10) (a) Rheingold, A. L.; DiMaio, A.-J. *Organometallics* **1986**, *5*, 393. (b) The ^1H NMR data published by West et al. show four upfield (uncoordinated $AsCH_3$) methyl group resonances and six downfield (coordinated $AsCH_3$) methyl group resonances, the ratio required for a cyclodecamer complex formulation.[1a] West did not state the solvent used in obtaining his NMR data; we have recorded ^1H NMR spectra in C_6D_6, $CDCl_3$, and Me_2SO-d_6 and have found differences among the spectra tentatively attributed to differing rates of dynamic processes. The spectrum obtained in Me_2SO-d_6 closely resembles that published by West. The complete analysis of the NMR data including both solid state and solution ^{13}C spectra will be the subject of a future paper.

(11) Hildebrandt, R. L.; Wieser, J. D.; Montgomery, L. K. *J. Am. Chem. Soc.* **1973**, *95*, 8598.

Table IV. Atomic Coordinates ($\times 10^4$) and Isotropic Thermal Parameters ($\mathrm{Å}^2 \times 10^3$) for **3**

	x	*y*	*z*	*U*
Mo(1)	8887 (1)	2206 (1)	−161 (1)	34(1)[a]
Mo(2)	6871 (1)	2718 (1)	203 (1)	33(1)[a]
As(1)	7318 (1)	1488 (1)	−29 (1)	37(1)[a]
As(2)	6129 (2)	826 (1)	−794 (1)	48(1)[a]
As(3)	5576 (1)	1672 (1)	−1613 (1)	42(1)[a]
As(4)	6247 (1)	2702 (1)	−1028 (1)	35(1)[a]
As(5)	7978 (1)	2675 (1)	−1276 (1)	38(1)[a]
As(6)	8083 (1)	3882 (1)	−1561 (1)	42(1)[a]
As(7)	8890 (1)	4329 (1)	−535 (1)	40(1)[a]
As(8)	8493 (1)	3413 (1)	156 (1)	34(1)[a]
O(1)	9850 (10)	1913 (7)	1241 (5)	68(5)[a]
O(2)	11086 (10)	2781 (8)	−170 (8)	92(7)[a]
O(3)	9811 (12)	840 (7)	−598 (8)	108(8)[a]
O(4)	7698 (11)	2442 (7)	1627 (5)	74(6)[a]
O(5)	4861 (11)	2192 (8)	620 (7)	88(7)[a]
O(6)	6069 (11)	4173 (7)	530 (8)	87(7)[a]
C(1)	9491 (13)	1998 (8)	732 (9)	49(7)[a]
C(2)	10282 (14)	2594 (9)	−196 (8)	49(7)[a]
C(3)	9439 (13)	1319 (10)	−454 (9)	61(8)[a]
C(4)	7395 (14)	2546 (9)	1095 (8)	50(7)[a]
C(5)	5570 (14)	2376 (9)	436 (8)	53(7)[a]
C(6)	6378 (14)	3658 (9)	392 (8)	49(5)
C(11)	8373 (7)	445 (6)	806 (5)	43(7)[a]
C(12)	8436	−73	1252	67(9)[a]
C(13)	7581	−245	1510	74(10)[a]
C(14)	6663	102	1323	73(9)[a]
C(15)	6600	621	877	52(7)[a]
C(16)	7455	793	618	41(5)[a]
C(21)	7500 (12)	−276 (7)	−832 (6)	83(10)[a]
C(22)	8221	−687	−1045	111(13)[a]
C(23)	8594	−509	−1587	119(14)[a]
C(24)	8244	81	−1916	89(11)[a]
C(25)	7522	492	−1702	66(9)[a]
C(26)	7150	314	−1160	89(8)[a]
C(31)	3468 (10)	1957 (6)	−1976 (5)	58(8)[a]
C(32)	2458	2086	−1917	70(9)[a]
C(33)	2165	2039	−1330	79(10)[a]
C(34)	2883	1864	−801	74(10)[a]
C(35)	3893	1735	−859	53(7)[a]
C(36)	4185	1782	−1447	46(7)[a]
C(41)	4971 (10)	3877 (7)	−1154 (4)	67(8)[a]
C(42)	4252	4346	−1445	81(10)[a]
C(43)	3901	4312	−2092	73(9)[a]
C(44)	4268	3808	−2449	74(9)[a]
C(45)	4987	3339	−2158	65(8)[a]
C(46)	5338	3373	−1511	40(5)[a]
C(51)	7309 (9)	2531 (7)	−2630 (7)	67 (9)[a]
C(52)	7427	2331	−3232	107 (13)[a]
C(53)	8263	1934	−3314	113 (14)[a]
C(54)	8981	1737	−2792	105 (13)[a]
C(55)	8863	1937	−2190	95 (12)[a]
C(56)	8027	2334	−2108	57 (8)[a]
C(61)	9104 (8)	3806 (7)	−2609 (5)	63 (8)[a]
C(62)	9915	3747	−2935	74 (9)[a]
C(63)	10908	3661	−2606	92 (12)[a]
C(64)	11090	3635	−1950	63 (8)[a]
C(65)	10279	3694	−1624	54 (8)[a]
C(66)	9286	3780	−1953	37 (6)[a]
C(71)	8100 (8)	5403 (6)	131 (5)	61 (8)[a]
C(72)	7419	5906	251	83 (10)[a]
C(73)	6486	5987	−154	76 (10)[a]
C(74)	6233	5566	−678	73 (9)[a]
C(75)	6914	5064	−798	66 (8)[a]
C(73)	7848	4983	−394	53 (8)[a]
C(81)	10263 (9)	3883 (6)	1050 (5)	62 (8)[a]
C(82)	10753	4213	1593	68 (9)[a]
C(83)	10181	4481	2017	78 (11)[a]
C(84)	9119	4420	1899	74 (9)[a]
C(85)	8629	4090	1356	58 (7)[a]
C(86)	9201	3822	932	38 (6)[a]

[a] Equivalent isotropic *U* defined as one-third of the trace of the orthogonalized U_{ij} tensor.

Table V. Selected Bond Distances, Angles, and Torsion Angles for **1**

(a) Bond Distances (Å)			
As(1)–Mo(1)	2.599 (1)	As(1)–As(3a)	2.431 (1)
As(2)–Mo(1)	2.590 (2)	As(2)–As(3)	2.444 (1)
As(1)–As(1b)	2.466 (2)		
(b) Bond Angles (deg)			
As(1)–Mo(1)–As(2)	88.4 (0)	C(2)–Mo(1)–C(2c)	89.5 (8)
As(1)–Mo(1)–As(1c)	93.5 (1)	As(1b)–As(1)–As(3a)	103.0 (1)
As(1)–Mo(1)–C(1)	92.3 (3)	As(3)–As(2)–As(3c)	92.8 (1)
As(1)–Mo(1)–C(2)	88.5 (4)	As(2)–As(3)–As(1a)	92.4 (1)
As(1)–Mo(1)–C(2c)	177.0 (3)	Mo(1)–As(1)–As(1b)	110.4 (0)
As(2)–Mo(1)–C(1)	178.9 (5)	Mo(1)–As(1)–As(3a)	117.3 (1)
As(2)–Mo(1)–C(2)	89.3 (3)	Mo(1)–As(2)–As(3)	120.9 (0)
C(1)–Mo(1)–C(2)	89.9 (5)		
(c) As Atom Torsion Angles (deg)			
2–3–1a–1c	45.7	3a–1–1b–3c	174.1
3c–2–3–1a	91.6		

Table VI. Selected Bond Distances, Angles, and Torsion Angles for **2**

(a) Bond Distances (Å)			
Mo(1)–As(1)	2.573 (3)	As(3)–As(4)	2.479 (4)
Mo(1)–As(4)	2.583 (3)	As(4)–As(5)	2.455 (4)
Mo(1)–As(7)	2.592 (3)	As(5)–As(6)	2.457 (4)
Mo(2)–As(3)	2.621 (3)	As(6)–As(7)	2.471 (4)
Mo(2)–As(6)	2.585 (3)	As(7)–As(8)	2.469 (4)
Mo(2)–As(9)	2.612 (3)	As(8)–As(9)	2.440 (4)
As(1)–As(2)	2.450 (4)	As(1)–As(9)	2.480 (4)
As(2)–As(3)	2.424 (3)		
(b) Bond Angles (deg)			
Mo(1)–As(1)–As(2)	119.2 (1)	As(7)–Mo(1)–C(3)	92.2 (9)
Mo(1)–As(1)–As(9)	110.1 (1)	C(1)–Mo(1)–C(2)	85.7 (11)
Mo(1)–As(4)–As(3)	110.8 (1)	C(1)–Mo(1)–C(3)	90.7 (11)
Mo(1)–As(4)–As(5)	118.4 (1)	C(2)–Mo(1)–C(3)	84.3 (11)
Mo(1)–As(7)–As(6)	110.3 (1)	As(3)–Mo(2)–C(4)	91.9 (8)
Mo(1)–As(7)–As(8)	117.5 (1)	As(3)–Mo(2)–C(5)	176.8 (7)
Mo(2)–As(3)–As(2)	106.0 (1)	As(3)–Mo(2)–C(6)	94.4 (8)
Mo(2)–As(3)–As(4)	108.6 (1)	As(6)–Mo(2)–C(4)	174.1 (7)
Mo(2)–As(6)–As(5)	106.8 (1)	As(6)–Mo(2)–C(5)	92.6 (9)
Mo(2)–As(6)–As(7)	109.5 (1)	As(6)–Mo(2)–C(6)	89.1 (8)
Mo(2)–As(9)–As(8)	106.1 (1)	As(9)–Mo(2)–C(4)	96.1 (7)
Mo(2)–As(9)–As(1)	109.8 (1)	As(9)–Mo(2)–C(5)	89.0 (8)
As(1)–Mo(1)–As(4)	88.6 (1)	As(9)–Mo(2)–C(6)	176.7 (7)
As(1)–Mo(1)–As(7)	89.4 (1)	C(4)–Mo(2)–C(5)	86.2 (12)
As(4)–Mo(1)–As(7)	88.8 (1)	C(4)–Mo(2)–C(6)	85.1 (10)
As(3)–Mo(2)–As(6)	89.5 (1)	C(5)–Mo(2)–C(6)	88.0 (11)
As(3)–Mo(2)–As(9)	88.7 (1)	As(1)–As(2)–As(3)	89.8 (1)
As(6)–Mo(2)–As(9)	89.7 (1)	As(2)–As(3)–As(4)	104.1 (1)
As(1)–Mo(1)–C(1)	87.7 (7)	As(3)–As(4)–As(5)	93.0 (1)
As(1)–Mo(1)–C(2)	95.7 (7)	As(4)–As(5)–As(6)	88.7 (1)
As(1)–Mo(1)–C(3)	178.4 (8)	As(5)–As(6)–As(7)	103.9 (1)
As(4)–Mo(1)–C(1)	96.5 (7)	As(6)–As(7)–As(8)	93.3 (1)
As(4)–Mo(1)–C(2)	175.2 (8)	As(7)–As(8)–As(9)	88.8 (1)
As(4)–Mo(1)–C(3)	91.4 (9)	As(8)–As(9)–As(1)	104.2 (1)
As(7)–Mo(1)–C(1)	173.9 (6)	As(9)–As(1)–As(2)	91.5 (1)
As(7)–Mo(1)–C(2)	89.2 (8)		
(c) As Atom Torsion Angles (deg)			
1–2–3–4	−47.6	6–7–8–9	−64.6
2–3–4–5	163.7	7–8–9–1	−49.8
3–4–5–6	−65.1	8–9–1–2	164.6
4–5–6–7	−49.1	9–1–2–3	−65.8
5–6–7–8	163.4		

The average As–As–As bond angle in **1** (96.1°) is considerably smaller than that in cyclodecane (116.7°). The metal atom coordination geometry is only slightly distorted from octahedral. The Mo atom environment is of the *fac*-[(Mo(CO)$_3$L$_3$] type and conforms to an 18-electron count. Each coordinated As atom functions as a two-electron donor. As seen in Figure 2, each of the Mo–As bonds is eclipsed by an Mo–C bond when viewed along the Mo⋯Mo vector. Attempts to convert **1** by both thermal and photochemical methods to discrete cluster forms failed. Only at temperatures above 240 °C did **1** show evidence of reaction, and only intractable products were formed.

However, when arsenobenzene, *cyclo*-(PhAs)$_6$, replaces arsenomethane in reactions with (mesitylene)Mo(CO)$_3$, several suc-

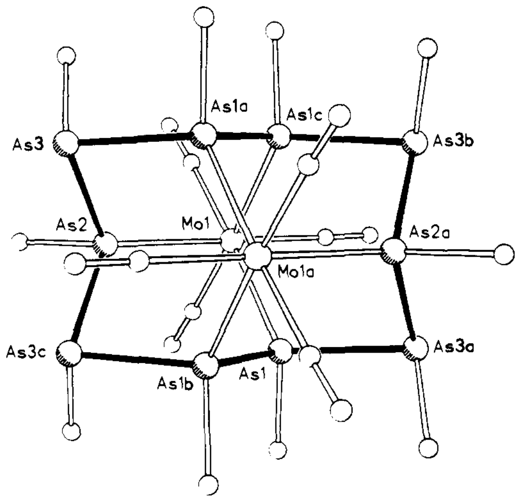

Figure 2. The structure of **1** as viewed along the Mo···Mo vector.

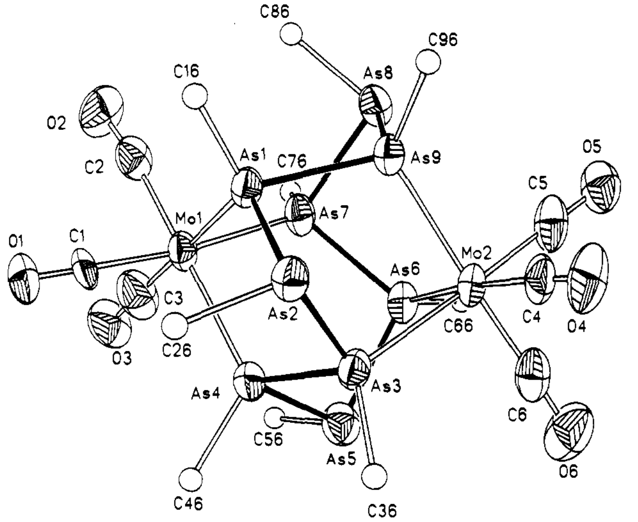

Figure 3. Molecular structure and labeling scheme for **2** with phenyl rings shown as ipso atoms of arbitrary radii.

cessive products may be obtained by incremental increase in the rigorousness of conditions. The product isolated after heating at 70 °C is a cyclononamer complex [*cyclo*-$(PhAs)_9Mo(CO)_6$] (**2**), which on heating to 120 °C (or directly from starting material at 120 °C) is converted to the Mo–Mo bonded catenaoctamer [*catena*-$(PhAs)_8Mo_2(CO)_6$] (**3**). **3** may be converted to the extensively rearranged diarsenido complex, **5**, on heating to 160 °C. **5** and other products of **3** will be detailed in a subsequent report.

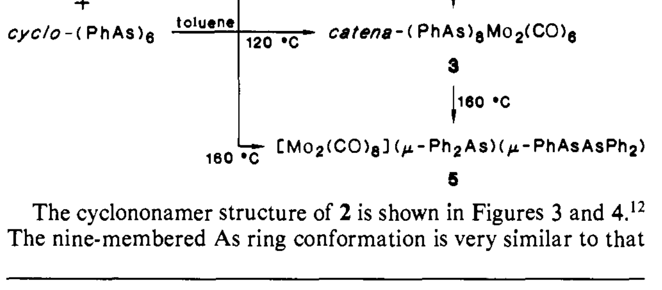

The cyclononamer structure of **2** is shown in Figures 3 and 4.[12] The nine-membered As ring conformation is very similar to that

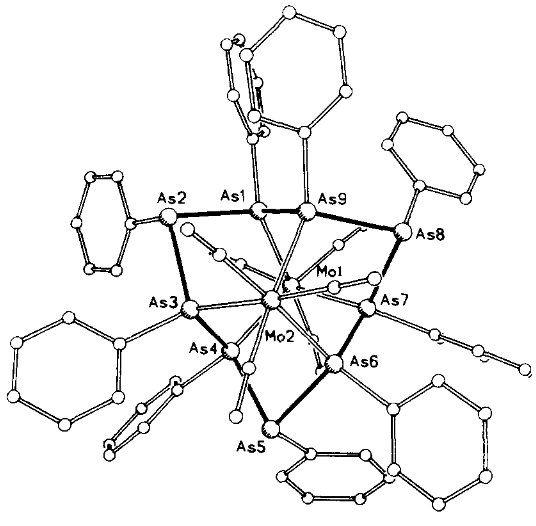

Figure 4. The structure of **2** viewed along the Mo···Mo vector.

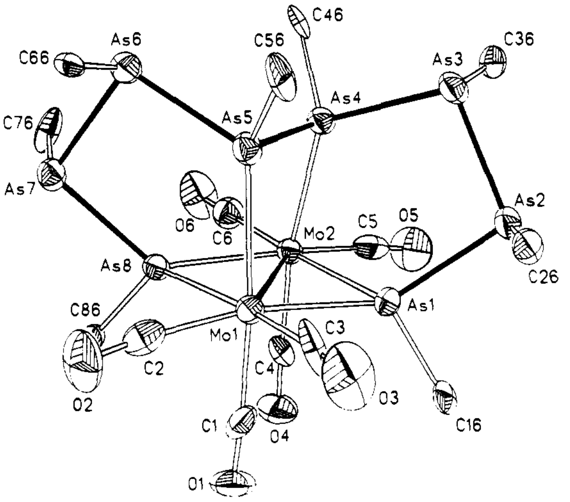

Figure 5. Molecular structure and labeling scheme for **3** with phenyl rings shown as ipso atoms only.

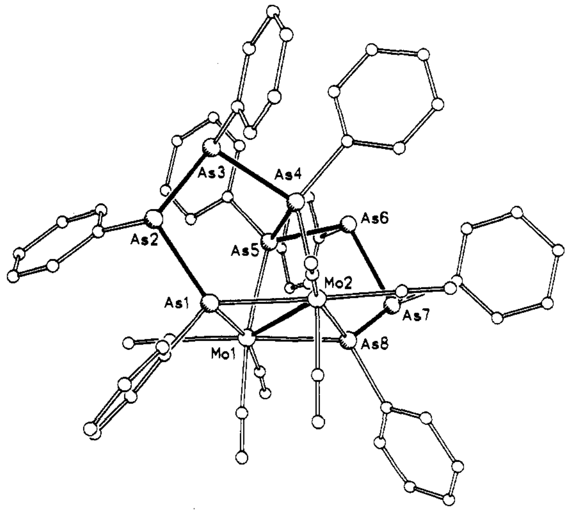

Figure 6. The structure of **3** viewed from a perspective that reveals the orientation of the phenyl ring planes.

found in cyclononylammonium bromide.[13] This conformation, from calculations, is one of two almost equal, minimum energy conformations. A closely related structure is found in [*cyclo*-$(CH_3As)_9Cr_2(CO)_6$].[1b] The metal atom geometry, as in **1**, is

---

[12] On crystallization from CH_2Cl_2, crystals of **2** containing CH_2Cl_2 are grown: monoclinic, $P2_1/n$, $a = 17.761$ (5) Å, $b = 18.883$ (5) Å, $c = 19.981$ (6) Å, $\beta = 94.85$ (3)°, $V = 6677$ (2) Å^3, $Z = 4$, $R_F = 7.20\%$. The two forms, with regard to the cluster, are chemically indistinguishable. The structure of the EtOH solvate of **2** produced more satisfactory results and is the one we report in detail.

[13] Dunitz, J. D.; Prelog, V. *Angew. Chem.* **1960**, *72*, 896.

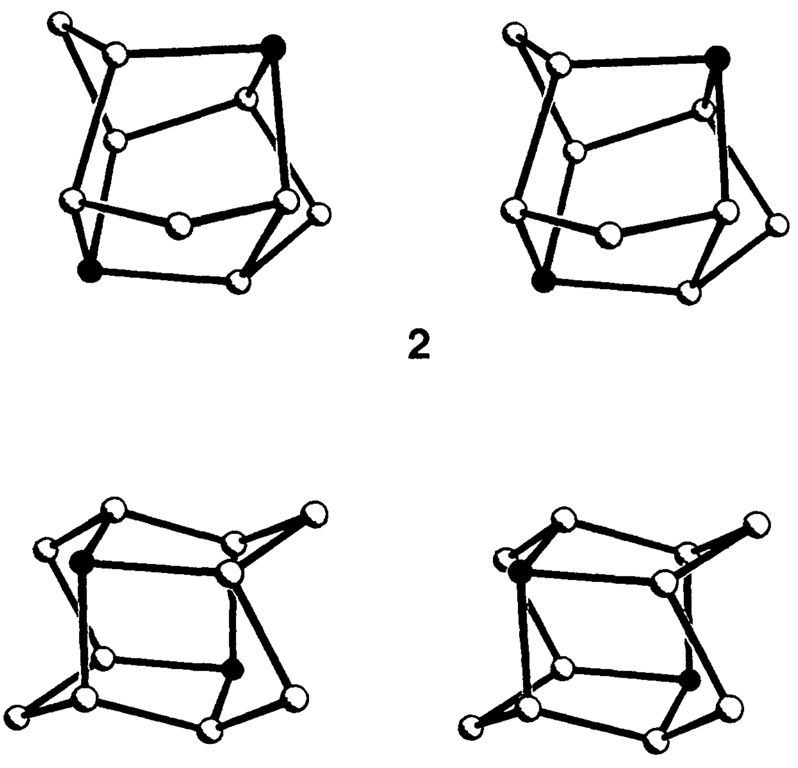

Figure 7. Stereoviews of the heavy-atom structures of **2** (top) and **1** (bottom).

nearly octahedral and also of the *fac*-[Mo(CO)$_3$L$_3$] type, although somewhat more distorted than found for **1**. The nine PhAs units form bonds to Mo at the 1, 3, 4, 6, 7, and 9 positions. The view in Figure 4 shows a staggering of Mo–As and Mo–C bonds; in **1** the same bonds are eclipsed. An Mo···Mo separation of 5.100 (3) Å indicates the absence of a metal–metal bond. The crowding of phenyl rings in the structure is shown by some fairly short H···H contacts, e.g., H(71)···H(61) = 2.46 Å (the shortest).

The structure of 3 is shown in Figures 5 and 6. A chain of eight PhAs units is metal coordinated at the 1, 4, 5, and 8 positions. Both terminal As atoms bridge both metal atoms. The metal–ligand framework resembles the better known bis(μ-diorganophosphido)dimolybdenum octacarbonyl complexes (e.g., [M(CO)$_4$]$_2$(μ-PEt$_2$)$_2$[14]). Unlike **1** and **2**, **3** contains an Mo–Mo bond, 3.094 (2) Å; in the related structure of [*catena*-(η-C$_3$H$_9$As)$_8$Mo$_2$(CO)$_6$], the Mo–Mo distance is 3.105 (5) Å.[1b] If the Mo–Mo bond is neglected, the metal atom geometry is still octahedral, but far more distorted than in either **1** or **2**, particularly in the angles forming the central As(1)As(8)Mo(1)Mo(2) rhombus, which is, itself, nearly planar (the dihedral angle folded at the Mo–Mo bond is 5.3°). The two best-fit planes formed from the atoms [As(1)As(2)As(3)As(4)] and [As(5)As(6)As(7)As(8)] are nearly perpendicular to the [Mo(1)Mo(2)As(4)As(5)] plane, the angles being 87.0 and 90.4°, respectively.

If the chain termini are regarded as three-electron donors, **3** also has an 18-electron metal atom environment.

Comparisons of the key structural parameters for **1–3** to other Mo–As catenate structures and the *cyclo*-(RAs)$_n$ precursors are given in Table VIII.

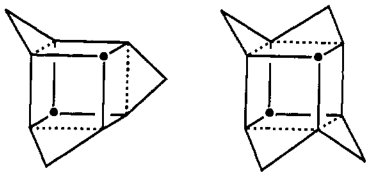

Figure 8. Idealized constructions of the cubane-derived heavy-atom structures of **2** (left) and **1** (right). The Mo atom positions are shown as solid circles.

Discussion

Most of the known transition-metal, main-group hybrid clusters contain more metallic atoms than non-metallic atoms in their cluster frameworks. It is not surprising, therefore, that many hybrid cluster structures represent perturbations of all-metal structures in which the non-metallic units serve as bridging, edge-capping, and face-capping units for various groupings of two–six metal atoms. Large transition-metal clusters of ten or more atoms generally approach *closo* structures in an approximation of bulk metal structures. In contrast, large clusters of the heavier main-group elements of groups 15 and 16 tend much more to form open structures similar to their allotropic forms.[15] In seeking precedent for the frameworks of structures **1–3** (considering both the As and Mo atoms), it has proved more successful to compare them to main-group analogues. The heavy-atom framework in **1** and **2** is shown in stereoviews in Figure 7, and also in idealized form in Figure 8. The structure of **2** is that of the known alicyclic hydrocarbon, trishomocubane,[16] which is also found in the P$_{11}$$^{3-}$ ion.[17] von Schnering has elegantly shown the structural relationship of P$_{11}$$^{3-}$ (and, therefore, also **2**) to a cubane system and provided predictions for other cubane-derived structures.[18] In trishomocubane, three cubane edges are opened and bridged by CH$_2$ groups to produce eight CH and three CH$_2$ vertices. The three CH$_2$ vertices correspond positionally to the three uncoordinated PhAs units in the nine-membered ring, and

---

(14) Nassimbeni, L. R. *Inorg. Nucl. Chem. Lett.* **1971**, *7*, 909.

(15) Wells, A. F. *Structural Inorganic Chemistry*, 5th ed.; Clarendon: Oxford, 1984.

(16) Underwood, G. R.; Ramamoorthy, B. *Tetrahedron Lett.* **1970**, 4125. Smith, E. C.; Barborak, J. C. *J. Org. Chem.* **1976**, *41*, 1433.

(17) Wichelhaus, W.; von Schnering, H.-G. *Naturwissenschaften* **1973**, *60*, 104.

(18) von Schnering, H.-G. In *Homoatomic Rings, Chains and Macromolecules of the Main-Group Elements*; Rheingold, A. L., Ed.; Elsevier: Amersterdam, 1977; p 317.

Table VII. Selected Bond Distances, Angles, and Torsion Angles for **3**

(a) Bonds Distances			
Mo(1)–Mo(2)	3.094 (2)	As(1)–As(2)	2.449 (2)
Mo(1)–As(1)	2.577 (2)	As(2)–As(3)	2.443 (3)
Mo(1)–As(5)	2.661 (2)	As(3)–As(4)	2.468 (2)
Mo(1)–As(8)	2.578 (2)	As(4)–As(5)	2.456 (3)
Mo(2)–As(1)	2.560 (2)	As(5)–As(6)	2.461 (2)
Mo(2)–As(4)	2.640 (2)	As(6)–As(7)	2.449 (2)
Mo(2)–As(8)	2.572 (2)	As(7)–As(8)	2.454 (2)
(b) Bond Angles (deg)			
Mo(1)–Mo(2)–As(1)	53.2 (1)	As(5)–Mo(1)–C(3)	98.5 (5)
Mo(1)–Mo(2)–As(4)	82.7 (1)	As(8)–Mo(1)–C(1)	90.0 (5)
Mo(1)–Mo(2)–As(8)	52.5 (1)	As(8)–Mo(1)–C(2)	84.0 (5)
Mo(1)–Mo(2)–C(4)	91.2 (6)	As(8)–Mo(1)–C(3)	169.6 (5)
Mo(1)–Mo(2)–C(5)	141.4 (5)	As(1)–Mo(2)–C(4)	88.5 (5)
Mo(1)–Mo(2)–C(6)	132.4 (5)	As(1)–Mo(2)–C(5)	88.5 (5)
Mo(2)–Mo(1)–As(1)	52.7 (1)	As(1)–Mo(2)–C(6)	174.4 (5)
Mo(2)–Mo(1)–As(5)	80.9 (1)	As(4)–Mo(2)–C(4)	168.9 (5)
Mo(2)–Mo(1)–As(8)	53.2 (1)	As(4)–Mo(2)–C(5)	96.8 (5)
Mo(2)–Mo(1)–C(1)	92.3 (5)	As(4)–Mo(2)–C(6)	99.2 (5)
Mo(2)–Mo(1)–C(2)	137.0 (5)	As(8)–Mo(2)–C(4)	88.7 (5)
Mo(2)–Mo(1)–C(3)	137.2 (5)	As(8)–Mo(2)–C(5)	163.2 (5)
Mo(1)–As(1)–Mo(2)	74.1 (1)	As(8)–Mo(2)–C(6)	80.1 (5)
Mo(1)–As(8)–Mo(2)	74.4 (1)	C(1)–Mo(1)–C(2)	84.2 (7)
As(1)–Mo(1)–As(5)	92.4 (1)	C(1)–Mo(1)–C(3)	90.9 (7)
As(1)–Mo(1)–As(8)	105.7 (1)	C(2)–Mo(1)–C(3)	85.8 (8)
As(5)–Mo(1)–A(8)	80.7 (1)	C(4)–Mo(2)–C(5)	82.1 (7)
As(1)–Mo(2)–As(4)	80.4 (1)	C(4)–Mo(2)–C(6)	91.8 (7)
As(1)–Mo(2)–As(8)	105.5 (1)	C(5)–Mo(2)–C(6)	86.1 (8)
As(4)–Mo(2)–As(8)	94.7 (1)	As(1)–As(2)–As(3)	101.7 (1)
As(1)–Mo(1)–C(1)	88.7 (5)	As(2)–As(3)–As(4)	98.8 (1)
As(1)–Mo(1)–C(2)	168.0 (5)	As(3)–As(4)–As(5)	97.9 (1)
As(1)–Mo(1)–C(3)	84.7 (5)	As(4)–As(5)–As(6)	97.5 (1)
As(5)–Mo(1)–C(1)	170.6 (5)	As(5)–As(6)–As(7)	98.9 (1)
As(5)–Mo(1)–C(2)	96.2 (5)	As(6)–As(7)–As(8)	100.3 (1)
(c) As Atom Torsion Angles (deg)			
1–2–3–4	−12.9	4–5–6–7	93.0
2–3–4–5	87.0	5–6–7–8	−19.7
3–4–5–6	133.5		

Table VIII. A Comparison of Bond Parameters in the Cyclic Precursors and Molybdenum Carbonyl Complexes of Catenated RAs Units

	av As–As (Å)	av As–As–As (deg)	av Mo–As (Å)	ref
cyclo-$(CH_3As)_5$	2.428	101.8		20
cyclo-$(PhAs)_6$	2.459	91.1		21
[*cyclo*-$(CH_3As)_{10}Mo_2(CO)_6$] (**1**)	2.447	96.1	2.595	this work
[*cyclo*-$(PhAs)_9Mo_2(CO)_6$] (**2**)	2.458	95.3	2.594	this work
[*catena*-$(PhAs)_8Mo_2(CO)_6$ (**3**)	2.454	99.2	2.598	this work
[*cyclo*-$(PhAs)_6Mo(CO)_4$]	2.454	98.6	2.618	5
[*catena*-$(CH_3As)_5$-$(\eta^5$-$C_5H_5)_2Mo_2(CO)_4$]	2.441	97.5	2.627	2a
[*catena*-$(C_3H_7As)_8Mo_2(CO)_6$]	NR[a]	NR	2.581	1b

[a] Not reported.

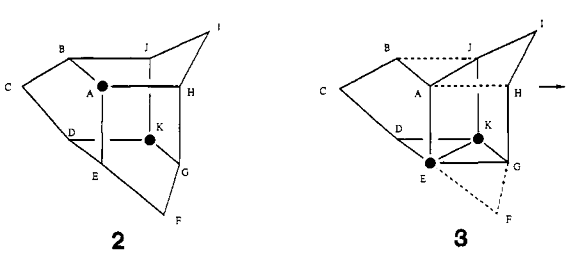

2 **3**

Figure 9. The conversion of **2** (left) to **3** may involve a conservation of the cubane-derived structure of **2**. The right-hand figure is a precursor to **3**; **3** is formed when H moves in the direction shown by the arrow.

the eight CH vertices correspond to the six, coordinated PhAs units plust the two $Mo(CO)_3$ groups. Clear isolobal relationships[19] exist between trishomocubane and **2**. The $Mo(CO)_3$ fragment may be viewed as an analogue of CH^{3+} if the three unligated octahedral orbitals are unoccupied, the uncoordinated PhAs units as CH_2 analogues and each of the six coordinated PhAs units as CH^- analogues. The assemblage of these eleven parts provides an electrically neutral molecule and emphasizes the donor/acceptor nature of complex formation. (The $P_{11}{}^{3-}$ ion may be decomposed to produce three P^- ions in the "flap" positions as CH^- analogues and the eight P vertices as CH analogues.)

The structures of **1** and **3** have no known hydrocarbon (or other compositional) analogues, but they are equally accessible by application of the same isolobal arguments developed for **2**. The structure of **1** also has a cubane-derived framework. A particularly curious aspect of the cubane-derived structures of **1** and **2** is that, if the $Mo(CO)_3$ groups are fixed at the ends of a body diagonal, the found structures for **1** and **2** represent the only symmetrical arrangements of "flap" positions for pentacycloundecane and pentacyclododecane analogues, respectively. Currently, no examples are known of coordinated rings of either eight or twelve RE units, but by extrapolation from these arguments, it may be predicted that the structure of a [*cyclo*-$(RE)_8Mo_2(CO)_6$] complex would involve a chair conformation of a cyclooctane analogue bonded through the 1, 2, 3, 5, 6, and 7 positions to form, in completion, a cubane-derived pentacyclodecane structure. Likewise, a [*cyclo*-$(RE)_{12}Mo_2(CO)_6$] structure would involve a cyclododecane ring coordinated in the 1, 3, 5, 7, 9, and 11 positions to form, overall, a pentacyclotetradecane structure. If a [*cyclo*-$(RE)_{11}Mo_2(CO)_6$] were prepared, it could not be structurally related to this series due to the lack of a possible symmetrical arrangement of five "flaps", if body-diagonal $Mo(CO)_3$ group placement is maintained; an unsymmetrical structure would, of course, still be possible. We are currently seeking the development of synthesis routes to coordinated rings of eight and twelve members by varying R, E, and the metal. Sterically demanding R groups may force smaller ring sizes, whereas large metal atoms such as found in $W(CO)_3$ and CpRe groups may accommodate larger ring sizes.

In the thermal conversion of **2** to **3**, it is intriguing to observe that the structure of **3** may be seen as a manipulation of the cubane-derived structure of **2**. Figure 9 shows the trishomocubane structure of **2** and a precursor to **3** which conserves several cubane structural elements. If *F* is the AsPh vertex eliminated on converting the *cyclo*-$(PhAs)_9$ system to *catena*-$(PhAs)_8$ and is replaced by the E–G bond, then breaking the B–J and A–H bond leaves the ABCDE ring free to rotate clockwise (as viewed) moving the Mo atom from A to E and positioning the rings for formation of the A–J and E–K bonds. Since H is no longer a cubane corner, it is free to move in the direction indicated by the arrow; the result is a heavy-atom framework remarkably similar to that shown in Figure 5. While such a process may be purely fanciful, the very high yield (73%) obtained when purified **2** is used to form **3** strongly supports an essentially intramolecular process involving some sequential variant of that described. The conversion of **2** to **3** may have as its driving force the increased donor capacity of the As_8 chain of **3** formed from the As_9 ring of **2**. Chain termini can be three-electron donors, whereas the maximum for ring members is two. It is reasonable, therefore, that the terminal AsPh units which bridge both atoms form a more stable system than the two-electron-donor As–Mo bonds formed by ring members (and interior members of chains). In accord with this, the terminal As–Mo distances in **3** are shorter (despite their bridging character) than those formed by the interior chain members: (average terminal) = 2.572 (2) Å and (average interior) = 2.651 (2) Å. The formation of the very long Mo–Mo bond in **3** is not likely a major factor in the overall energy change for the rearrangement, although its presence may be a factor in the charge-delocalizing

---

(19) Hoffmann, R. *Angew. Chem., Int. Ed. Engl.* **1982**, *21*, 711. Stone, F. G. A. *Angew. Chem., Int. Ed. Engl.* **1984**, 23, 89.

(20) Burns, J. H.; Waser, J. *J. Am. Chem. Soc.* **1957**, *79*, 859.

(21) Rheingold, A. L.; Sullivan, P. J. *Organometallics* **1983**, *2*, 327.

potential of the As_2Mo_2 rhombus.

Acknowledgment. The authors are grateful to R. Hoffmann for a helpful discussion about the isolobal relationships. Support for this work was obtained, in part, from the University of Delaware Center for Catalytic Science and Technology and from the donors of the Petroleum Research Fund, administered by the American Chemical Society.

Supplementary Material Available: Complete listings of bond distances and angles, anisotropic temperature coefficients, and hydrogen atom coordinates for **1**, **2**, and **3** (13 pages); listing of observed and calculated structure factors for **1–3** (56 pages). Ordering information is given on any current masthead page.

Synthesis, Characterization, and Reactivity of α-Ketoacyl Complexes of Platinum(II) and Palladium(II). Crystal Structures of *trans*-$Pt(PPh_3)_2(Cl)(COCOPh)$ and *cis*-$Pt(PPh_3)_2(COPh)(COOMe)$

Ayusman Sen,*[1] Jwu-Ting Chen,[2a] William M. Vetter, and Robert R. Whittle[2b]

Contribution from the Chandlee Laboratory, Department of Chemistry, Pennsylvania State University, University Park, Pennsylvania 16802. *Received May 14, 1986*

Abstract: The α-ketoacyl chloro complexes, *trans*-$M(PPh_3)_2(Cl)(COCOR)$ (M = Pt: R = Ph, **1a**; R = *p*-FC_6H_4, **1b**; R = *p*-ClC_6H_4, **1c**; R = *p*-MeC_6H_4, **1d**; R = Me, **1e**. M = Pd: R = Ph, **2**), were synthesized by the oxidative addition of the appropriate α-ketoacyl chloride with either $Pt(PPh_3)_4$ or $Pd(PPh_3)_4$. The crystal structure of **1a** showed a square-planar geometry around the Pt with the two carbonyl groups virtually coplanar and in an s-trans configuration. The above compounds were found to decompose thermally to the corresponding benzoyl compounds, *trans*-$M(PPh_3)_2(Cl)(COR)$. A detailed kinetic study of the decarbonylation of **1a** and **2** indicated the presence of two competing pathways, one of which involved the initial dissociation of a PPh_3 ligand. The kinetic and thermodynamic parameters for the various steps in the mechanism were determined. For the decarbonylation of compounds **1a–d**, a correlation was observed between the rate constant for the phosphine-independent pathway and σ_{para}. The cationic α-ketoacyl complexes, *trans*-$Pt(PPh_3)_2(L)(COCOR)^+BF_4^-$ (R = Ph: L = CH_3CN, **4a**; L = CO, **4b**; L = PPh_3, **4c**. R = Me: L = CH_3CN, **4d**), were prepared by Cl^- abstraction from the corresponding neutral compounds in the presence of an appropriate ligand. In the absence of any added ligand, the Cl^- abstraction from **1a** resulted in rapid deinsertion of CO to form *cis*-$Pt(PPh_3)_2(CO)(COPh)^+$ (**5a**) initially, which then slowly converted to the corresponding trans compound, **5b**. The decarbonylation of **1a** to the corresponding chloro benzoyl compound was catalyzed by the addition of **5b**. The addition of OMe^- to **5a** and **5b** resulted in the formation of the acyl–alkoxycarbonyl complexes *cis*- and *trans*-$Pt(PPh_3)_2(COPh)(COOMe)$, **6a** and **6b**, respectively. Similarly, *trans*-$Pt(PPh_3)_2(COCOPh)(COOMe)$ (**6d**) was formed by the reaction of OMe^- with **4b**. The crystal structure of **6a** revealed a square-planar geometry around the Pt with the COPh and COOMe groups lying in planes perpendicular to the plane of the molecule.

The 1,2-shift of alkyl and aryl groups between a metal center and the carbon atom of a coordinated CO molecule (eq 1) is frequently observed and is a well-studied reaction.[3] In contrast, the corresponding migration of an acyl group from the metal to the CO ligand (eq 2) has never been observed. The reverse


(1)

$$M\begin{matrix}\diagup CO\\ \diagdown R\end{matrix} \rightleftharpoons M—COR \quad (1)$$

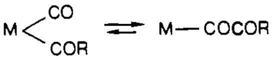
(2)

$$M\begin{matrix}\diagup CO\\ \diagdown COR\end{matrix} \rightleftharpoons M—COCOR \quad (2)$$

reaction, although known,[4,5] remains poorly defined from a mechanistic standpoint, mainly due to the paucity of well-characterized α-ketoacyl compounds.[4–6] Herein, we describe the synthesis and characterization of a family of neutral and cationic Pt(II) and Pd(II) α-ketoacyl compounds. We also report the results of our studies on the mechanism of acyl migration from a coordinated CO to the metal center. Our studies have allowed

Scheme I

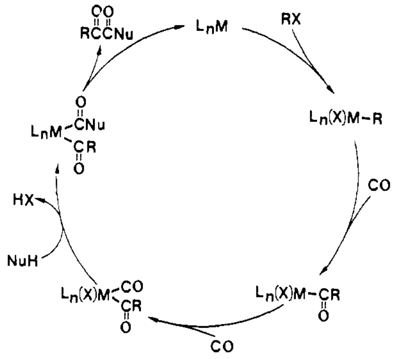

---

[1] Alfred P. Sloan Research Fellow, 1984–1986.

[2] (a) Current address: Department of Chemistry, National Taiwan University, Taipei, Taiwan, ROC. (b) X-ray crystallography.

[3] (a) Kochi, J. K. *Organometallic Mechanisms and Catalysis*; Academic: New York, 1978; Chapter 18. (b) Collman, J. P.; Hegedus, L. S. *Principles and Applications of Organotransition Metal Chemistry*; University Science Books: Mill Valley, CA, 1980; Chapter 5. (c) For reactions involving group 10 metals in particular, see: Anderson, G. K.; Cross, R. J. *Acc. Chem. Res.* **1984**, *17*, 67.

[4] (a) Casey, C. P.; Bunnell, C. A.; Calabrese, J. C. *J. Am. Chem. Soc.* **1976**, *98*, 1166. (b) Ozawa, F.; Sugimoto, T.; Yamamoto, T.; Yamamoto, A. *Organometallics* **1984**, *3*, 692.

[5] Chen, J.-T.; Sen, A. *J. Am. Chem. Soc.* **1984**, *106*, 1506.

[6] (a) Blake, D. M.; Vinson, A.; Dye, R. *J. Organomet. Chem.* **1981**, *204*, 257. (b) Selover, J. C.; Vaughn, G. D.; Strouse, C. E.; Gladysz, J. A. *J. Am. Chem. Soc.* **1986**, *108*, 1455. (c) For the synthesis of alkoxalyl complexes, see: Dobrzynski, E. D.; Angelici, R. J. *Inorg. Chem.* **1975**, *14*, 59. Fayos, J.; Dobrzynski, E.; Angelici, R. J.; Clardy, J. *J. Organomet. Chem.* **1973**, *59*, C33.

0002-7863/87/1509-0148$01.50/0